Synopsis

Name of Student: Anwesha Kanjilal

Department: Materials Engineering, Indian Institute of Science, Bangalore 560012, India

Title of Thesis: Effect of Length Scale on High Temperature Mechanical Behavior of Sn-Cu Joints: A Mechanics and Material Science Based Treatment

---

Miniaturization of microelectronic chips has paved the way for 3D stacking of dies with the help of miniature Pb-free Sn-rich solder joints in the interconnects. With progressive downscaling of the solder joint size, the volume of compliant Sn, which is the major component in the joints, has significantly reduced and the proportion of brittle intermetallic phases has increased. Moreover, the microscale joints have become highly constrained to deform due to their geometry and the stiffness mismatch of compliant Sn relative to the rigid substrates. Additionally, the statistical distribution of the number and orientation of the anisotropic Sn grains as well as the size and distribution of second-phase precipitates vary with decrease in the length scale of joints. Thus, a knowledge of the mechanical behaviour of bulk Sn or the solder alloys cannot be directly extended to accurately predict the response of the miniature Sn-Cu joints. So far separate studies have been conducted to understand the behavior in the bulk and the joints independently. However, attempts to bridge the gap over a wide length scale has been complicated due to inconsistency in the microstructure of Sn and dimensional constraints imposed by the geometry of the joint. This has resulted in lack of consensus in literature on the mechanical behavior of Sn-rich solder joints in both sample and microstructural length scales. Hence, the primary objective of this thesis is to develop a fundamental understanding of the effect of reduction in the dimensional and microstructural length scales on the high temperature mechanical behaviour of Sn-Cu joints in a

unified manner. The insights obtained from Sn-Cu joints have been applied to explain the behavior of SAC-Cu joints, which form a technologically important system.

The above mentioned problem has been addressed by first developing a preliminary understanding of the mechanical behaviour of bulk unconstrained materials of pure Sn and Sn rich Sn-Ag-Cu (SAC) solder alloys, followed by shrinking the size of Sn and solder from the bulk to miniature joints. The bulk Sn and SAC alloys were prepared by melting, from which a series of Sn-Cu and SAC-Cu joints were fabricated using diffusion bonding technique. The thickness of the joints was reduced from 1.4 mm to 170 μm. Continuum analysis based studies have shown that a multiaxial stress state is developed in joints that are fabricated using a compliant metal sandwiched between rigid substrates, and the magnitude of triaxiality depends on the thickness of the metal layer. Accordingly, the effect of change in the macroscopic stress state on the tensile and creep deformation as well as failure of the Sn-Cu joints was examined, and the accompanying role of microstructure was deconvoluted from the continuum effects.

At first, the size effect on the room temperature mechanical properties was determined by performing tensile tests on bulk Sn and the Sn-Cu joints. Room temperature is 0.59 and $0.6T_m$ for Sn and Sn-rich solder alloys, respectively. Hence, they qualify as high temperatures. The tensile strength and strain hardening exponent increased and the ductility decreased with reduction in joint thickness (see **Fig. 1(a)**). In addition to the strengthening imparted by the multiaxial stress state in the joints, crystal plasticity analysis revealed that increase in dislocation density due to constraints arising from Cu substrates also contributes to the higher tensile strength and hardening in thinner joints (see **Fig. 1(b)**). The effect of constraints on the deformation profile across the joint thickness and the mode of failure was clearly evident from tensile tests performed *in-situ* inside scanning electron microscope on different joint sizes.

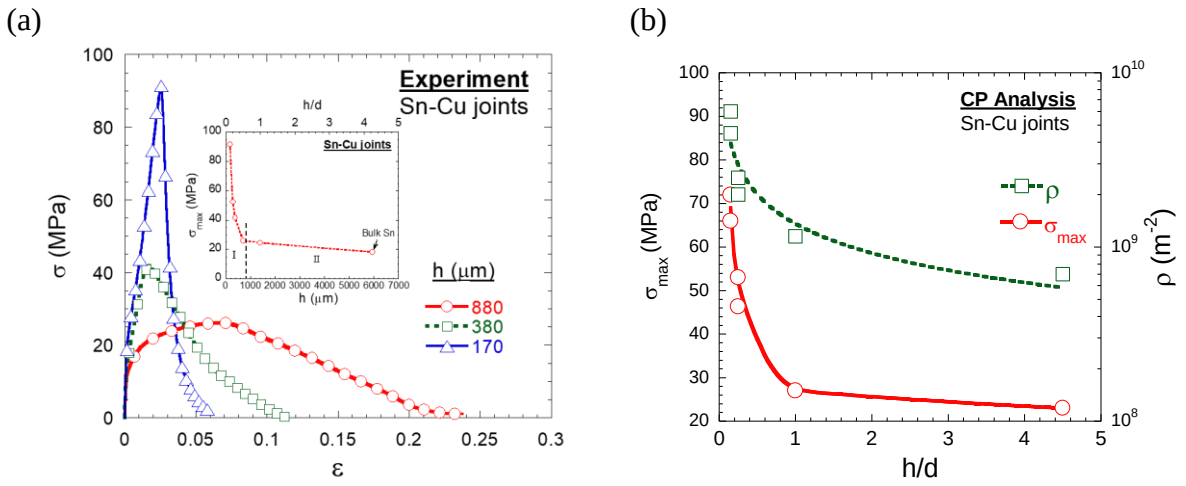

Fig. 1: Effect of joint thickness on tensile deformation of Sn-Cu joints: (a) Experimental results of the stress-strain behavior of different joint thicknesses; the inset shows the variation of maximum stress, σ_{max}, (obtained from the stress-strain curves) as a function of joint thickness, *h*, and aspect ratio, *h/d* and (b) crystal plasticity (CP) analysis of the effect of joint aspect ratio (and equivalently the joint thickness) on the maximum stress in the joints and the dislocation density, ρ.

This was followed by investigation of the effect of length scale on the creep behavior of joints. Both the secondary and the tertiary creep behavior were studied. At first, the creep behaviour of bulk Sn and Sn-Ag-Cu (SAC) solder alloys was investigated over a range of temperature to resolve the existing discrepancy in the creep parameters, i.e., activation energy, Q_c, and stress exponent, *n*. The creep rate decreased with increasing Ag content. However, irrespective of the composition, the creep mechanism was dislocation climb controlled by core diffusion at temperatures less than 150 ^oC and lattice diffusion at temperatures higher than 150 ^oC with Q_c and *n* changing from 55 kJ/mol and 7 to 100 kJ/mol and 5, respectively (**see Fig. 2**).

(a)

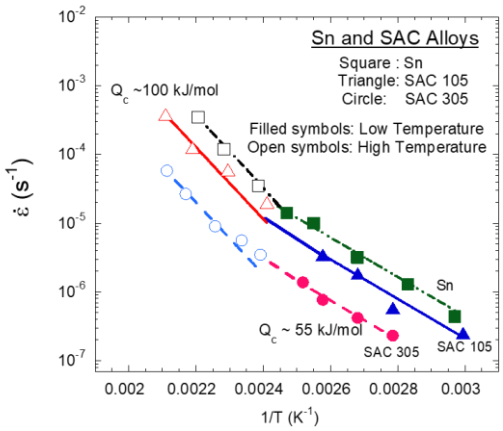

(b)

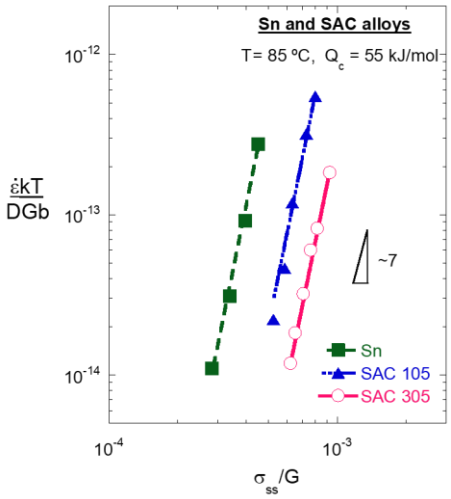

(c)

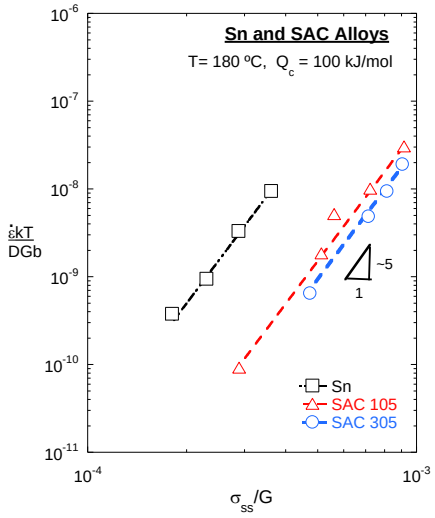

Fig. 2: Creep behavior of bulk unconstrained Sn and SAC alloys: (a) Arrhenius plot showing variation of steady state strain rate of pure Sn, SAC 105 and SAC 305 with inverse of temperature, used to calculate activation energy, Q_c, for creep, which is noted in the plot. Variation of normalized steady state strain rate with normalized stress for pure Sn, SAC 105 and SAC 305 alloys at (b) 85 ºC and (c) 180 ºC. The value of stress exponent is mentioned in each graph. The curve fitting parameter, *R*, is equal to 0.99 for all the three materials from (a)-(c).

Subsequently, for Sn-Cu joints it was observed that at a given applied stress, the secondary creep rate decreased by three orders of magnitude with an order of magnitude decrease in the joint size (see **Fig. 3**). However, a change in creep mechanism was not evident in the joints, as the stress exponent was similar to that of bulk Sn. Finite element (FE) analysis using continuum formulations attributed this strengthening to the geometric constraints imposed by Cu, which reduces the effective stress (i.e., von Mises stress) in Sn. While FE results were in close agreement with experiment in thick joints, it significantly over predicted the creep rate of miniature joints (see **Fig.**

4). To understand the above discrepancy between FE analysis and experiments, crystal plasticity (CP) creep modeling of Sn-Cu joints was performed by incorporating this microstructural length scale, in addition to the geometric constraints. CP simulations revealed that orientation anisotropy of Sn and the constraints imposed by substrates on the dislocation motion further reduces the creep rate in the miniature joints (see **Fig. 5**). It should be noted that orientation imaging also revealed that microstructure varied with length scale, from bulk Sn with multiple grains to miniature joints having a few grains. Using the insights from FE and CP modeling, a unified length scale sensitive model, incorporating both geometrical and microstructural factors, was developed which can accurately predict the secondary creep rate of the Sn-Cu joints. Similar aspects of joint size dependent strengthening were operative in the SAC-Cu joints, where additional strengthening occurred due to presence of precipitates.

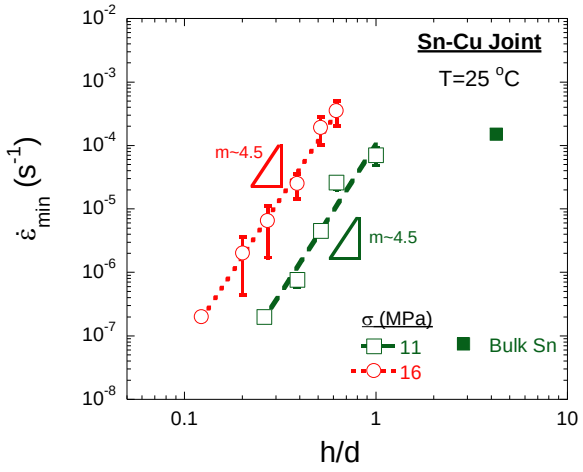

Fig. 3: Variation of minimum creep rate, $\dot{\varepsilon}_{min}$, with joint aspect ratio *h/d* (and equivalently joint thickness, *h*) at different applied stress. The dashed and dotted lines are the best fit curves representing the power law dependence of creep rate on joint size at 11 and 16 MPa, respectively. The slope of the curve in each case has been indicated. The error bars indicate the standard deviation from the corresponding average value obtained from tests repeated at respective data points.

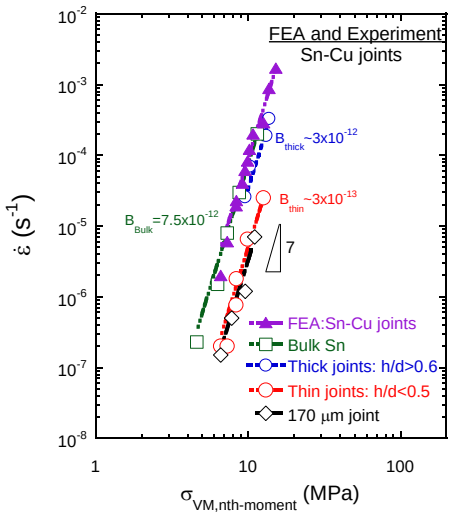

Fig. 4: Comparison of FEA and experimental results of variation of secondary creep rates as a function of average von Mises stress ($\sigma_{VM,nth-moment}$) for bulk Sn and Sn-Cu joints of different thickness. The solid symbols represent FE results and open symbols represent experimental data. The values of the prefactor *B* in the Norton power-law which was fitted to the curves are given next to each joint size rage. The value of the curve fitting parameter *R* is 0.99.

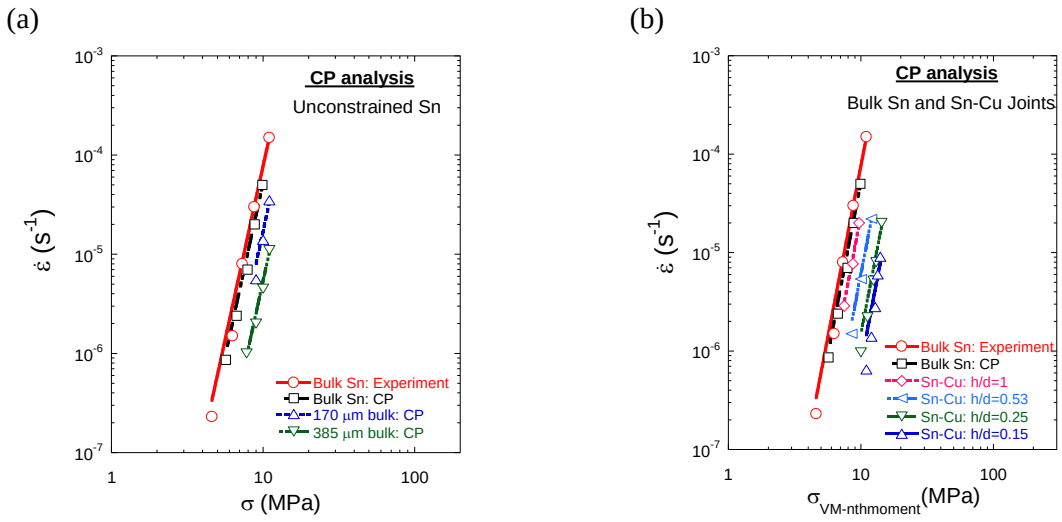

Fig. 5: Crystal plasticity simulation results showing (a) effect of crystal orientation and number of grains in Sn (representative of different joint thickness) on creep of bulk unconstrained Sn and comparison with experimental result and (b) effect of joint thickness, in terms of *h/d* ratio, on the strain rate versus n^{th} moment average of von Mises stress plot.

The tertiary creep of bulk Sn and SAC alloy exhibited two distinct stages, wherein the strain rate increased slowly in the first stage and rapidly in the second stage. The strain at which this transition occurred between the two stages, denoted as ε_{knee}, was independent of the applied

stress in pure Sn, which exhibited failure only by necking (see **Fig. 6(a)**). However, the transition strain decreased with stress in SAC alloy, which underwent extensive cavitation at precipitate-matrix interface along with necking (see **Fig. 6(a)**). On the contrary, the joints exhibited a single stage monotonous increase in the tertiary creep rate with increase in strain. However, for a given applied stress the value of tertiary creep rate and the amount of strain accumulated during tertiary decreased with reduction in joint size (see **Fig. 6(b)**). Microscopic examination of the fracture surfaces of the Sn layer in the joints revealed a transition in the mode of creep failure over the length scale, from pure necking in thick joints to cavitation along with constrained necking in thin joints.

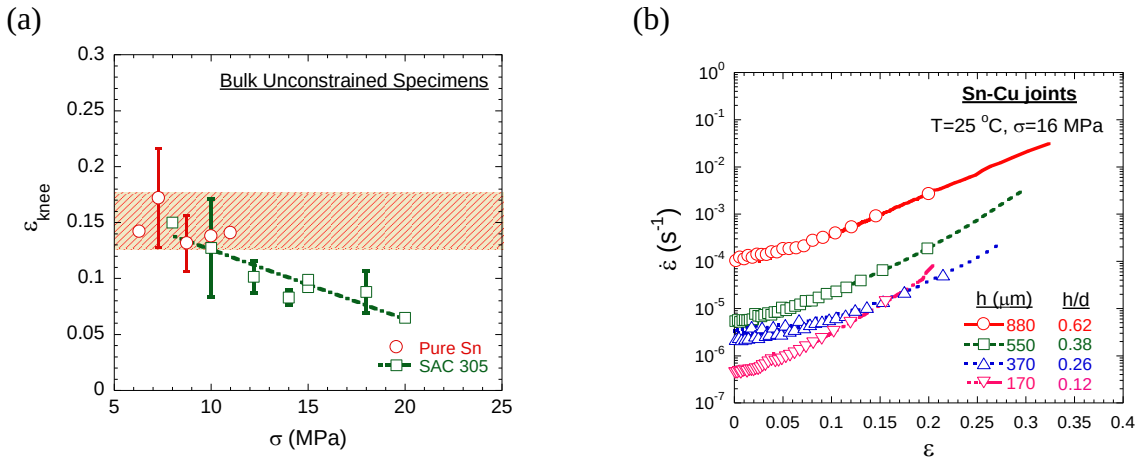

Fig. 6: Tertiary creep behavior of bulk Sn and SAC 305 and the Sn-Cu joints: (a) Variation of the transition strain, ε_{knee}, with stress in bulk Sn and SAC 305; the error bars in (a) indicate the standard deviation from average value obtained from multiple tests at the same stress. (b) Variation of tertiary creep rate with strain of Sn-Cu joints of different thickness and aspect ratio at an applied stress of 16 MPa.

The above mentioned differences in tertiary creep of both bulk metals and the joints were explained with the help of a mechanistic joint size dependent necking-cum-cavitation based tertiary creep model that can capture the effect of cavity growth on necking under uniaxial and multiaxial stress state during power law creep. The model predicted that the transition strain

between the two stages of tertiary in bulk material marks the onset of strain localization in the neck due to rapid neck growth or cavity growth. The model also showed a decrease in the transition strain with decrease stress if cavitation occurs with necking (see **Fig. 7(a)**). Furthermore, the model predicted that smaller size of the neck and higher triaxiality in thin joints decrease the tertiary creep strain and enhance the strain due to cavity growth while reducing that due to necking (see **Fig. 7(b)** and **(c)**).

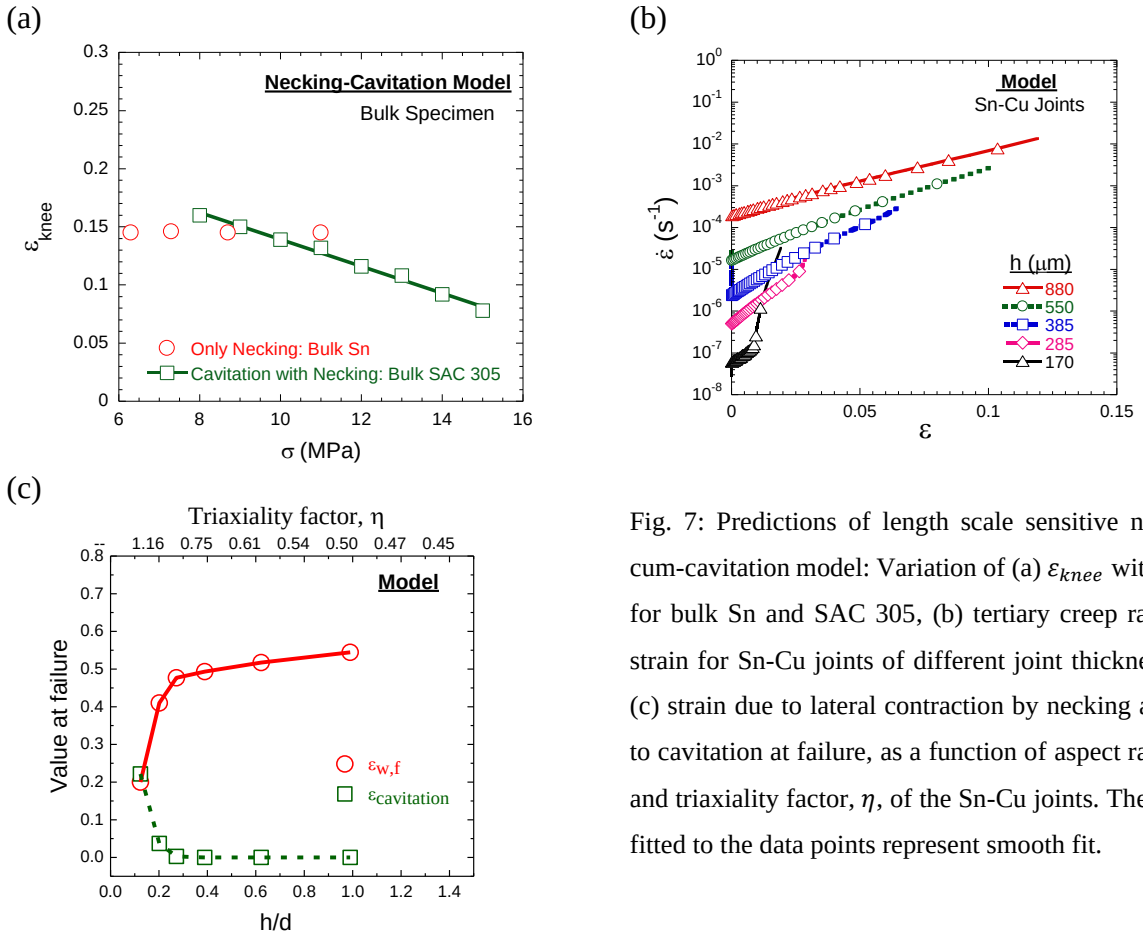

Fig. 7: Predictions of length scale sensitive necking-cum-cavitation model: Variation of (a) ε_{knee} with stress for bulk Sn and SAC 305, (b) tertiary creep rate with strain for Sn-Cu joints of different joint thickness, and (c) strain due to lateral contraction by necking and due to cavitation at failure, as a function of aspect ratio, *h/d* and triaxiality factor, η, of the Sn-Cu joints. The curves fitted to the data points represent smooth fit.

Overall, a systematic change in the tensile and creep strength and the mode of failure was evident with reduction in the length scale from bulk Sn to the thin Sn-Cu joints, which had contributions from both geometrical effect of varying stress state and microstructural effect of varying Sn orientation, composition and effect of constraints on dislocation motion.